J Sci Comput (2010) 43: 326–342
DOI 10.1007/s10915-008-9259-8

Stabilization by Local Projection for Convection–Diffusion and Incompressible Flow Problems

Sashikumaar Ganesan · Lutz Tobiska

Received: 30 October 2007 / Revised: 21 July 2008 / Accepted: 1 December 2008 /
Published online: 18 December 2008

Abstract We give a survey on recent developments of stabilization methods based on local projection type. The considered class of problems covers scalar convection–diffusion equations, the Stokes problem and the linearized Navier–Stokes equations. A new link of local projection to the streamline diffusion method is shown. Numerical tests for different type of boundary layers arising in convection–diffusion problems illustrate the stabilizing properties of the method.

Keywords Convection–diffusion equations · Incompressible flows · Local projection stabilization · Finite elements · Boundary layers

1 Introduction

It is well-known that standard finite element discretizations applied to convection–diffusion or incompressible flow problems show spurious oscillations in the case of higher Reynolds numbers due to dominating convection. A first systematic way to overcome this problem has started 30 years ago with the fundamental work [26] by developing a special discretization of advective terms. This idea of upwind finite elements has been developed in different ways and led to stable (low order) discretizations for the incompressible Navier–Stokes equations [22–25, 27]. Five years later the idea of streamline upwind Petrov–Galerkin (SUPG) stabilization has been proposed for the advective term in [8] and analyzed for a scalar convection–diffusion equation in [21]. The method is based on adding weighted residuals to the standard weak formulation to enhance stability without losing consistency. It turns out that this method is also able to handle another instability phenomena arising in incompressible flow problems, the instability of equal order interpolations for velocity and pressure.

S. Ganesan (✉) · L. Tobiska
Institute for Analysis and Computational Mathematics, Department of Mathematics, Otto von Guericke University, PF4120, 39016 Magdeburg, Germany
e-mail: ga.sashikumaar@ovgu.de

L. Tobiska
e-mail: tobiska@ovgu.de

The SUPG stabilization was extended to the Stokes problem in [19] where a pressure stabilization Petrov–Galerkin (PSPG) method is considered accommodating low equal-order interpolation to be stable and convergent. A detailed error analysis of these SUPG/PSPG-type stabilizations applied to the incompressible Navier–Stokes equations, including both the case of inf-sup stable and equal-order interpolations, can be found in [29]. Despite the progress of the SUPG/PSPG method in theory and application, an essential drawback of this method is—in particular for higher order interpolations—that various terms need to be added to the weak formulation to guarantee the consistency of the method in a strong way (Galerkin orthogonality holds for smooth solutions).

Over the last years, several approaches have been developed to relax the strong coupling of velocity and pressure in SUPG/PSPG-type stabilizations and to introduce symmetric versions of the stabilizing terms, we mention in particular the edge stabilization or continuous interior penalty (CIP) method [9–12] and the local projection stabilization (LPS) [2–4, 16, 20], for a general overview on stabilized schemes see [5].

The LPS is based on a projection $\pi_h : Y_h \to D_h$ of the finite element space Y_h into a discontinuous space D_h. Stabilization is achieved by adding terms which give a weighted L^2-control over the fluctuations $(id - \pi_h)$ of the gradients of the quantity of interest. This method has been introduced for the Stokes problem in [2], extended to the transport equation in [3], and analyzed for low order discretizations of the Oseen equations in [4]. As figured out in [20], the key idea in the error analysis of the local projection scheme is the construction of an interpolant into Y_h which exhibits an additional orthogonality property with respect to the projection space D_h. The existence of such an interpolation can be proven if the spaces Y_h and D_h satisfy a local inf-sup condition [16, 20]. In [2–4], a two-level approach has been used where the projection space D_h lives on a coarser mesh compared to the approximation space Y_h. An alternative technique of enriching the approximation space Y_h has been proposed in [20] which circumvents the disadvantage of the classical two-level form of the local projection scheme producing a stencil being less compact than for the SUPG/PSPG-type stabilization. In the CIP method, stabilization is achieved by adding a weighted L^2 control over the jumps of the derivatives leading also to a less being compact stencil as it has been the case for the two-level variant of the LPS. Because of this reason we restrict ourself to the LPS with enriched ansatz spaces and discuss its application to different problems in the following sections.

2 Local Projection Stabilization

Let $\mathcal{T}_h$ be a shape regular decomposition of the domain Ω into d-dimensional simplices, quadrilaterals or hexahedra. The diameter of a cell K will be denoted by h_K and the mesh parameter h represents the maximum diameter of the cells $K \in \mathcal{T}_h$. Let $Y_h \subset H^1(\Omega)$ be a finite element space of continuous, piecewise polynomial functions defined over $\mathcal{T}_h$. Let D_h denote a discontinuous finite element space defined on $\mathcal{T}_h$ and $D_h(K) := \{q_h|_K : q_h \in D_h\}$. Further, let $\pi_K : L^2(K) \to D_h(K)$ be a local projection which defines the global projection $\pi_h : L^2(\Omega) \to D_h$ by $(\pi_h w)|_K := \pi_K(w|_K)$. Associated with the projection π_h is the fluctuation operator $\kappa_h : L^2(\Omega) \to L^2(\Omega)$ defined by $\kappa_h := id - \pi_h$, where $id : L^2(\Omega) \to L^2(\Omega)$ is the identity. We will apply these operators also to vector-valued functions in a componentwise manner.

Assumption A1 There is an interpolation operator $j_h : H^1(\Omega) \to Y_h$ satisfying for all $q_h \in D_h$ and for all $w \in H^1(\Omega)$

$$(w - j_h w, q_h) = 0, \tag{1}$$

and for all $w \in H^l(\omega(K))$, $1 \le l \le r+1$, for all $K \in \mathcal{T}_h$

$$\|w - j_h w\|_{0,E} \le C\, h_K^{l-1/2} \|w\|_{l,\omega(K)}, \quad E \subset \partial K, \tag{2}$$

$$\|w - j_h w\|_{0,K} + h_K |w - j_h w|_{1,K} \le C\, h_K^{l} \|w\|_{l,\omega(K)}, \tag{3}$$

where $\omega(K)$ denotes a certain neighbourhood of the cell K which appears in the definition of interpolation operators for non-smooth functions.

Note that (2) and (3) describe the usual approximation properties, however, (1) is an additional orthogonality property. It has been proven in [20], that for spaces Y_h, D_h, satisfying the local inf-sup condition, i.e., there is a positive constant β_1 independent of h such that $\forall K \in \mathcal{T}_h$:

$$\inf_{q_h \in D_h(K)} \sup_{v_h \in Y_h(K)} \frac{(v_h, q_h)_K}{\|v_h\|_{0,K}\, \|q_h\|_{0,K}} \ge \beta_1 > 0, \tag{4}$$

a given interpolation satisfying (2), (3) can be modified in such a way that (1)–(3) hold. Here, $Y_h(K) := \{w_h|_K : w_h \in Y_h,\ w_h = 0 \text{ on } \Omega \backslash K\}$.

Assumption A2 Let the fluctuation operator κ_h satisfy the following approximation property:

$$\|\kappa_h q\|_{0,K} \le C\, h_K^{l} |q|_{l,K} \quad \forall q \in H^l(K),\ \forall K \in \mathcal{T}_h,\ 0 \le l \le r. \tag{5}$$

It is clear that $Y_h(K)$—compared to $D_h(K)$—has to be rich enough for satisfying (4). In particular, a necessary requirement is

$$\dim Y_h(K) \ge \dim D_h(K). \tag{6}$$

On the other hand D_h has to be large enough to guarantee A2. In the enriched version of the LPS both requirements are satisfied by enriching the approximation space Y_h for a given projection space D_h.

3 Convection–Diffusion Equation

We consider the convection–diffusion-reaction type problem

$$-\varepsilon \Delta u + b \cdot \nabla u + cu = f \quad \text{in } \Omega, \qquad u = u_D \quad \text{on } \Gamma_D, \qquad \varepsilon \partial_n u = g \quad \text{on } \Gamma_N \tag{7}$$

where $\partial\Omega = \Gamma_D \cup \Gamma_N$, $\Gamma_D \cap \Gamma_N = \emptyset$, n is the outer unit normal, the data b, c, f, u_D, g are sufficiently smooth, and $0 < \varepsilon \ll 1$ is a given small positive parameter. We assume that the inflow part of the boundary $\Gamma_- := \{x \in \partial\Omega : b(x) \cdot n(x) < 0\}$ is a subset of Γ_D and that

$$c - \frac{1}{2} \operatorname{div} b \ge c_0 > 0.$$

Let us assume that $V_0 := \{v \in H^1(\Omega) : v|_{\Gamma_D} = 0\}$ and $\tilde{u}_D \in H^1(\Omega)$ denotes an extension of the Dirichlet data $u_D \in H^{1/2}(\Gamma_D)$. Then, a weak formulation of (7) reads:

Find $u \in \tilde{u}_D + V_0$ such that for all $v \in V_0$

$$a(u, v) := \varepsilon(\nabla u, \nabla v) + (b \cdot \nabla u + cu, v) = (f, v) + \langle g, v \rangle_{\Gamma_N}. \tag{8}$$

Integration by parts leads to

$$a(v,v) \geq \varepsilon |v|_1^2 + c_0 \|v\|_0^2 + \frac{1}{2}\langle |b\cdot n|, v^2\rangle_{\Gamma_N} \quad \forall v \in V_0,$$

and applying the Lax–Milgram lemma gives the unique solvability of the problem (8). Let $V_{0,h} = Y_h \cap V_0$. The associated stabilized discrete problem reads:

Find $u_h \in \tilde{u}_{D,h} + V_{0,h}$ such that for all $v_h \in V_{0,h}$

$$\varepsilon(\nabla u_h, \nabla v_h) + (b\cdot\nabla u_h + c u_h, v_h) + S_h(u_h, v_h) = (f, v_h) + \langle g, v_h\rangle_{\Gamma_N} \tag{9}$$

where $\tilde{u}_{D,h} = j_h \tilde{u}_D$ is an approximation of the Dirichlet data and S_h denotes the stabilizing term given by

$$S_h(u_h, v_h) := \sum_{K\in\mathcal{T}_h} \tau_K \big(\kappa_h(b\cdot\nabla)u_h, \kappa_h(b\cdot\nabla)v_h\big)_{0,K}.$$

Note that there is a close relation to the stabilization by subgrid modeling [13, 18] as discussed in [20]. However, in the subgrid modeling gradients of fluctuations instead of fluctuations of gradients are used. Associated with the discrete bilinear form A_h, we introduce the mesh-dependent norm

$$|||v||| := \left(\varepsilon |v|_1^2 + c_0\|v\|_0^2 + \frac{1}{2}\langle |b\cdot n|, v^2\rangle_{\Gamma_N} + \sum_{K\in\mathcal{T}_h} \tau_K \|\kappa_h(b\cdot\nabla)v\|_{0,K}^2\right)^{1/2}. \tag{10}$$

Theorem 3.1 *Assume A1, A2, and $\tau_K \sim h_K$. Then, there is a positive constant C independent of ε such that*

$$|||u - u_h||| \leq C\,(\varepsilon^{1/2} + h^{1/2}) h^r |u|_{r+1}.$$

Sketch of proof The proof follows the general line of showing the coercivity of the underlying discrete bilinear form and estimating the consistency as well as the approximation error. It is similar to the proof given in [3] for the hyperbolic transport problem ($\varepsilon = 0$, $\Gamma_N = \emptyset$, $\Gamma_D = \Gamma_-$, two-level approach). The tricky part is the estimation of the convection term which splits into three terms

$$\begin{aligned}(b\cdot\nabla(j_h u - u), w_h) = &-(j_h u - u, b\cdot\nabla w_h) - (\operatorname{div} b(j_h u - u), w_h)\\ &+ \langle b\cdot n(j_h u - u), w_h\rangle_{\Gamma_N}\end{aligned}$$

using integration by parts. For the first term we use the orthogonality and approximation properties of the special interpolant and $\tau_K \sim h_K$ to get

$$\begin{aligned}\big|(j_h u - u, b\cdot\nabla w_h)\big| &= \big|(j_h u - u, \kappa_h(b\cdot\nabla)w_h)\big|\\ &\leq C\left(\sum_{K\in\mathcal{T}_h} \tau_K^{-1} h_K^{2r+2} |u|_{r+1,K}^2\right)^{1/2}\left(\sum_{K\in\mathcal{T}_h} \tau_K \|\kappa_h(b\cdot\nabla)w_h\|_{0,K}^2\right)^{1/2},\\ &\leq C\, h^{r+1/2}|u|_{r+1}\,|||\, w_h\,|||\,.\end{aligned}$$

The estimation of the second and third term uses the approximation properties and the definition of the 'triple' norm

$$\big|(\operatorname{div} b(j_h u - u), w_h)\big| \leq C h^{r+1}|u|_{r+1}\|w_h\|_0 \leq C h^{r+1}|u|_{r+1}\,|||\, w_h|||,$$

$$\begin{aligned}\left|\langle b\cdot n(j_h u-u), w_h\rangle_{\Gamma_N}\right| &\le \| \, |b\cdot n|^{1/2}(j_h u-u)\|_{0,\Gamma_N} \, \| \, |b\cdot n|^{1/2} w_h\|_{0,\Gamma_N}\\ &\le Ch^{r+1/2}|u|_{r+1} \, |||\, w_h \, |||\,.\end{aligned}$$

Combining with standard estimates yields the stated error estimate. □

We give examples of pairs of finite element spaces (Y_h, D_h) satisfying the assumptions of Theorem 3.1. Let $F_K : \widehat{K} \to K$ be the mapping from the reference cell $\widehat{K}$ onto a cell $K \in \mathcal{T}_h$, P_s denote the space of all polynomials of degree less than or equal to s, and Q_s denote the space of all polynomials of degree less than or equal to s in each variable. We consider mapped finite element spaces

$$\begin{aligned}Y_h &:= \{v_h \in H^1(\Omega) : v_h|_K \circ F_K \in \widehat{Y}\},\\ D_h &:= \{q_h \in L^2(\Omega) : q_h|_K \circ F_K \in \widehat{D}\}.\end{aligned}$$

On simplicial meshes we can take $(P_r^{\text{bubble}}, P_{r-1}^{\text{disc}})$, which means with barycentric coordinates λ_i

$$\widehat{Y} := P_r + \left(\prod_{i=1}^{d+1}\lambda_i\right) P_{r-1}, \qquad \widehat{D} := P_{r-1}.$$

On quadrilateral/hexahdral meshes the pair $(Q_r^{\text{bubble}}, P_{r-1}^{\text{disc}})$ satisfies the requirements of Theorem 3.1 [20], more precisely

$$\widehat{Y} := Q_r \oplus \operatorname{span}\left(\left(\prod_{i=1}^{d}(1-\xi_i^2)\right)\xi_i^{r-1}; i=1,\ldots,d,\right), \qquad \widehat{D} := P_{r-1}.$$

4 Relationship to the SUPG Method

It is well-known that starting with the standard Galerkin piecewise linear finite element method on simplices enriched by cubic bubbles and eliminating the bubble part yields the SUPG method [1, 7]. Moreover, the shape of the bubble defines the SUPG-parameter uniquely, but the symmetric version of the bubble

$$\varphi_K(x) := \prod_{i=1}^{d+1}\lambda_i^K, \quad \lambda_i^K\text{—barycentric coordinates of } K,$$

generates the SUPG-parameter for the diffusion dominated and not for the convection dominated case. Several approaches have been developed to overcome this problem, reaching from the pseudo-residual-free [6] up to the residual free-bubble method [15] where the bubbles are local solutions of the problem under consideration. In the following, we will show that by starting with the LPS instead of the standard Galerkin approach and eliminating the symmetric bubble the SUPG method with the correct SUPG-parameter in both the diffusion dominated and the convection dominated case can be recovered.

Let us consider the problem (7) with piecewise constant functions b and f, and with $c = 0$, $\Gamma_D = \partial\Omega$, $u_D = 0$. We consider the case where $V_h = Y_h \cap H_0^1(\Omega)$ consists of piecewise linear functions and enrich this space by a bubble space B_h defined by

$$B_h := \operatorname{span}\{\varphi_K, \ \forall K \in \mathcal{T}_h\}. \tag{11}$$

Now we consider the local projection method on the enriched space $V_h \oplus B_h$ where the projection space is the space of discontinuous, piecewise constant functions:

Find $u_h \in V_h \oplus B_h$ such that for all $v_h \in V_h \oplus B_h$,

$$\varepsilon(\nabla u_h, \nabla v_h) + (b \cdot \nabla u_h, v_h) + S_h(u_h, v_h) = (f, v_h). \tag{12}$$

The dimension of the corresponding algebraic system of equations can be reduced by static condensation of the bubble part of the solution. To do this we write the solution u_h as $u_h = u_L + u_B$, with $u_L \in V_h$ and $u_B \in B_h$, and use the test functions $v_h = v_L \in V_h$ and $v_h = v_B \in B_h$. Taking into consideration that ∇v_L is piecewise constant, we get $\kappa_h(b \cdot \nabla)v_L = 0$ for all $v_L \in V_h$. Hence (12) can be reformulated as:

Find $u_L \in V_h$ and $u_B \in B_h$ such that for all $v_L \in V_h$ and all $v_B \in B_h$,

$$\varepsilon(\nabla(u_L + u_B), \nabla v_L) + (b \cdot \nabla(u_L + u_B), v_L) = (f, v_L), \tag{13}$$

$$\varepsilon(\nabla(u_L + u_B), \nabla v_B) + (b \cdot \nabla(u_L + u_B), v_B) + S_h(u_B, v_B) = (f, v_B). \tag{14}$$

Now from the representation

$$u_B = \sum_{K \in \mathcal{T}_h} d_K \varphi_K,$$

where the d_K are unknown constants, we obtain from the second equation:

Given $u_L \in V_h$, find $\{d_K : d_K \in \mathbb{R}\}$ such that for each K,

$$\varepsilon(\nabla(u_L + d_K\varphi_K), \nabla\varphi_K)_K + (b \cdot \nabla(u_L + d_K\varphi_K), \varphi_K)_K + S_h(d_K\varphi_K, \varphi_K) = (f, \varphi_K)_K. \tag{15}$$

Integrating by parts gives us

$$(\nabla u_L, \nabla\varphi_K)_K = -(\Delta u_L, \varphi_K)_K + \left\langle \frac{\partial u_L}{\partial n}, \varphi_K \right\rangle_{\partial K} = 0,$$

$$d_K(b \cdot \nabla\varphi_K, \varphi_K)_K = \frac{d_K}{2} \langle b \cdot n, \varphi_K^2 \rangle_{\partial K} = 0,$$

$$\pi_h(b \cdot \nabla)\varphi_K = \frac{1}{|K|} b \cdot \int_K \nabla\varphi_K \, dx = \frac{1}{|K|} b \cdot \int_{\partial K} \varphi_K \, n \, d\gamma = 0$$

and (15) reduces to:

Given $u_L \in V_h$, find $\{d_K : d_K \in \mathbb{R}\}$ such that for each K,

$$d_K\left(\varepsilon|\varphi_K|_{1,K}^2 + \tau_K\|b \cdot \nabla\varphi_K\|_{0,K}^2\right) = (f - b \cdot \nabla u_L, \varphi_K)_K$$

with the solution

$$d_K = \frac{(1, \varphi_K)_K}{\varepsilon|\varphi_K|_{1,K}^2 + \tau_K\|b \cdot \nabla\varphi_K\|_{0,K}^2} (f - b \cdot \nabla u_L)\big|_K. \tag{16}$$

Observing that $\varepsilon(\nabla u_B, \nabla v_L) = 0$ (see above), we reduce (13) to

$$\varepsilon(\nabla u_L, \nabla v_L) + (b \cdot \nabla u_L, v_L) + \sum_{K \in \mathcal{T}_h} d_K(b \cdot \nabla\varphi_K, v_L)_K = (f, v_L). \tag{17}$$

The term $\sum_{K\in\mathcal{T}_h}\cdots$ does not appear in the standard Galerkin finite element method applied on the space V_h. It can be rewritten as

$$\sum_{K\in\mathcal{T}_h} d_K(b\cdot\nabla\varphi_K, v_L)_K = -\sum_{K\in\mathcal{T}_h} d_K(b\cdot\nabla v_L, \varphi_K)_K$$
$$= \sum_{K\in\mathcal{T}_h} \gamma_K(b\cdot\nabla u_L - f, b\cdot\nabla v_L)_K,$$

where

$$\gamma_K = \frac{1}{|K|}\frac{|(1,\varphi_K)_K|^2}{\varepsilon|\varphi_K|^2_{1,K} + \tau_K\|b\cdot\nabla\varphi_K\|^2_{0,K}}. \tag{18}$$

We have now eliminated the bubble part from (12), arriving at

$$\varepsilon(\nabla u_L, \nabla v_L) + (b\cdot\nabla u_L, v_L) + \sum_{K\in\mathcal{T}_h}\gamma_K(b\cdot\nabla u_L, b\cdot\nabla v_L)_K$$
$$= (f, v_L) + \sum_{K\in\mathcal{T}_h}\gamma_K(f, b\cdot\nabla v_L)_K, \tag{19}$$

for all $v_L\in V_h$. This is the SUPG method with the SUPG-parameter γ_K given by (18). A scaling argument shows $(1,\varphi_K)\sim|K|$, $|\varphi_K|^2_{1,K}\sim|K|/h_K^2$, and $\|b\cdot\nabla\varphi_K\|^2_{0,K}\sim|K|\,\|b\|^2/h_K^2$, which means that γ_K behaves like $\gamma_K\sim h_K^2/(\varepsilon+\tau_K\|b\|^2)$. For $\tau_K=0$, we get $\gamma_K\sim h_K^2/\varepsilon$ which corresponds to the diffusion dominated case. Now γ_K is decreasing for increasing τ_K. The choice $\gamma_K\sim h_K/\|b\|$ in the convection dominated case $\|b\|\,h_K/\varepsilon\gg 1$ corresponds to $\tau_K\sim h_K/\|b\|$. Increasing τ_K further, in particular let $\tau_K\to\infty$, then we end up with the standard Galerkin approach corresponding $\gamma_K=0$. This interesting effect of the influence of stabilizing the higher modes (cubic bubbles by local projection) to the lower modes (piecewise linear finite elements) can be detected also from our numerical tests in the last section.

5 Stokes Problem

We will see that the general idea of local projection stabilization can be used to stabilize equal order interpolations. Let $V := (H_0^1(\Omega))^d$ and $Q := L_0^2(\Omega)$. A weak formulation of the Stokes problem reads:

Find $(u,p)\in V\times Q$ such that

$$(\nabla u,\nabla v) - (p,\operatorname{div} v) + (q,\operatorname{div} u) = (f,v)\quad\forall(v,q)\in V\times Q. \tag{20}$$

The Lax–Milgram theorem applied to the subspace of divergence-free functions and the inf-sup condition

$$\inf_{q\in Q}\sup_{v\in V}\frac{(q,\operatorname{div} v)}{\|q\|_0\,|v|_1} > 0, \tag{21}$$

guarantee that there is a unique solution of (20), see [17]. Equal order interpolations are introduced, i.e. $V_h := (Y_h\cap H_0^1(\Omega))^d$ and $Q_h := Y_h\cap L_0^2(\Omega)$. Circumventing the discrete version of (21), we consider the stabilized discrete problem:

Find $(u_h, p_h) \in V_h \times Q_h$ such that for all $(v_h, q_h) \in V_h \times Q_h$

$$(\nabla u_h, \nabla v_h) - (p_h, \operatorname{div} v_h) + (q_h, \operatorname{div} u_h) + S_h(p_h, q_h) = (f, v_h), \tag{22}$$

with the stabilization term

$$S_h(p_h, q_h) := \sum_{K \in \mathcal{T}_h} \alpha_K \left(\kappa_h \nabla p_h, \kappa_h \nabla q_h\right)_K \tag{23}$$

where α_K are parameters to be chosen. The error will be measured in the mesh-dependent norm

$$|||(v, q)|||_{ST} := \left(|v|_1^2 + \|q\|_0^2 + \sum_{K \in \mathcal{T}_h} \alpha_K \|\kappa_h \nabla q\|_{0,K}^2 \right)^{1/2}. \tag{24}$$

Theorem 5.1 *Assume $\alpha_K \sim h_K^2$, A1, and A2 with r replaced by $r-1$. Then, there exists a positive constant C independent of h such that*

$$|||(u - u_h, p - p_h)|||_{ST} \leq C\, h^r \left(\|u\|_{r+1} + \|p\|_r\right).$$

Proof For a complete proof we refer to [16]. Let us discuss the parameter choice $\alpha_K \sim h_K^2$ in more detail. The property that the interpolation error of the velocity is orthogonal to the projection space D_h is used to estimate the term

$$\begin{aligned} |(q_h, \operatorname{div}(u - j_h u))| &= |(\nabla q_h, (u - j_h u))| = |(\kappa_h \nabla q_h, (u - j_h u))| \\ &\leq C \left(\sum_{K \in \mathcal{T}_h} \alpha_K^{-1} h_K^{2(r+1)} \|u\|_{r+1,K} \right)^{1/2} |||(v_h, q_h)|||. \end{aligned}$$

The consistency error caused by adding the stabilization term $S_h(\cdot, \cdot)$ to the standard Galerkin discretization becomes for $p \in H^r(\Omega)$

$$\sup_{(v_h, q_h) \in V_h \times Q_h} \frac{|S_h(p, q_h)|}{|||(v_h, q_h)|||} \leq C \left(\sum_{K \in \mathcal{T}_h} \alpha_K h_K^{2(r-1)} |\nabla p|_{r-1,K}^2 \right)^{1/2}.$$

We see from these inequalities that $\alpha_K \sim h_K^2$ is the optimal choice. □

Remark As in the previous section we could assume that the projection space has been chosen such that A2 with r not replaced by $r-1$ is satisfied. An example would be the pair $(Y_h, D_h) = (P_1^{\text{bubble}}, P_0)$, satisfying A1 and A2 for $r = 1$. Then, for higher regularity of the pressure, $p \in H^{r+1}$, the consistency error becomes

$$\sup_{(v_h, q_h) \in V_h \times Q_h} \frac{|S_h(p, q_h)|}{|||(v_h, q_h)|||} \leq C \left(\sum_{K \in \mathcal{T}_h} \alpha_K h_K^{2r} |\nabla p|_{r,K}^2 \right)^{1/2}$$

and with $\alpha_K \sim h_K$ we would expect a $O(h^{r+1/2})$ error estimate. However, due to the presents of the $|\cdot|_1$ norm in the $|||\cdot|||$ norm the convergence order is restricted to r under Assumptions A1 and A2. Indeed, the full range $c_1 h_K^2 \leq \alpha_K \leq 1$ leads to a $O(h^r)$ error estimate [16].

Note that using the pair $(Y_h, D_h) = (P_1^{\text{bubble}}, P_0)$ and (22) means to approximate the velocity components and the pressure by functions belonging to P_1^{bubble}, i.e. $V_h = (P_1^{\text{bubble}})^d$ and $Q_h = P_1^{\text{bubble}}$. This differs from the Mini element discretization where $V_h = (P_1^{\text{bubble}})^d$ and $Q_h = P_1$ and no stabilization term is needed. However, in both cases we can eliminate the bubble part and end up with the stabilized method studied in [19] with and without an grad-div stabilization also used in [14]. We refer to [16] for more details.

The relaxed assumption A2 (r replaced by $r-1$) in Theorem 5.1 allows more freedom in the choice of the approximation and projection space, respectively. For example, a possible choice on simplicial meshes is $(Y_h, D_h) = (P_r^{\text{bubble}}, P_{r-2}^{\text{disc}})$, $r \geq 2$, with the modified bubble space

$$\widehat{Y} := P_r + \left(\prod_{i=1}^{d+1} \lambda_i\right) P_{r-2}.$$

On quadrilateral or hexahedral meshes the pair $(Y_h, D_h) = (Q_r, Q_{r-2}^{\text{disc}})$, with $r \geq 2$, of standard finite element spaces satisfies all assumptions of Theorem 5.1 Further examples and numerical tests can be found in [16].

6 Oseen Equation

Consider the linearized Navier–Stokes equations after a semi-implicit time discretization in a weak formulation:

$$\text{Find } (u, p) \in V \times Q: \qquad A\big((u, p); (v, q)\big) = (f, v) \quad \forall (v, q) \in V \times Q$$

where $V := H_0^1(\Omega)^d$, $Q := L_0^2(\Omega)$, $\nu > 0$, $\sigma \geq 0$, $b \in W^{1,\infty}(\Omega)$, $\operatorname{div} b = 0$, and the bilinear form $A(\cdot, \cdot)$ on the product space $V \times Q$ is given by

$$A\big((u, p); (v, q)\big) := \nu(\nabla u, \nabla v) + \big((b \cdot \nabla)u, v\big) + \sigma(u, v) - (p, \nabla \cdot v) + (q, \nabla \cdot u).$$

The stabilized problem is now generated by adding

$$S_h\big((u_h, p_h); (v_h, q_h)\big) := \sum_{K \in \mathcal{T}_h} \big[\tau_K \big(\kappa_h((b \cdot \nabla)u_h), \kappa_h((b \cdot \nabla)v_h)\big)_K + \mu_K \big(\kappa_h(\nabla \cdot u_h), \kappa_h(\nabla \cdot v_h)\big)_K + \alpha_K (\kappa_h \nabla p_h, \kappa_h \nabla q_h)_K\big]$$

with user-chosen parameters τ_K, μ_K, and α_K to the left hand side, thus we get:

Find $(u_h, p_h) \in V_h \times Q_h$ such that for all $(v_h, q_h) \in V_h \times Q_h$

$$(A + S)\big((u_h, p_h); (v_h, q_h)\big) = (f, v_h)$$

where $V_h := (Y_h \cap H_0^1(\Omega))^d$ and $Q_h := Y_h \cap L_0^2(\Omega)$. Now, the mesh-dependent norm becomes

$$|||(v, q)|||_{OS} := \big(\nu |v|_1^2 + \sigma \|v\|_0^2 + (\nu + \sigma)\|q\|_0^2 + S_h\big((v, q); (v, q)\big)\big)^{1/2}.$$

Theorem 6.1 *Assume A1, A2, $\tau_K \sim h_K$, $\mu_K \sim h_K$, and $\alpha_K \sim h_K$. Then, there exists a positive constant C independent of h such that*

$$|||(u - u_h, p - p_h)|||_{OS} \leq C(\nu^{1/2} + h^{1/2}) h^r \big(\|u\|_{r+1} + \|p\|_{r+1}\big).$$

Proof Note that different to Theorem 5.1, we assumed a higher regularity of the pressure to get the $O(h^{r+1/2})$ error estimate for $\nu < h$. For more details see [20]. □

7 Numerical Tests

This section presents the numerical results for the convection diffusion equation where the discretization is stabilized with the local projection method. In particular, the numerical results for the first order finite element P_1^{bubble} with projection onto P_0, and the second order finite element P_2^{bubble} with projection onto P_1^{disc} on triangles are presented. To demonstrate the robustness of the local projection method, we considered different examples with inner and boundary layers. Further, to show the effect of the stabilization on the lower modes, all images in our figures are generated using only the solution of P_1 (piecewise linear) part.

7.1 Example 1

Let $\Omega = (0,1)^2$, $\epsilon = 10^{-8}$, $b = (2,3)^{\mathrm{T}}$, $c = 1$ and $\Gamma_N := \emptyset$ be in (7). The right-hand side f and the Dirichlet data u_D are chosen in such a way that

$$u(x,y) = xy^2 - y^2 \exp\left(\frac{2(x-1)}{\epsilon}\right) - x \exp\left(\frac{3(y-1)}{\epsilon}\right) + \exp\left(\frac{2(x-1)+3(y-1)}{\epsilon}\right)$$

be the solution of (7). This example is having layers at the outflow boundary part.

In this example, we triangulate the square domain with 8,192 triangular cells. This results in 12,417 and 41,217 degrees of freedom for P_1^{bubble} and P_2^{bubble} elements, respectively. The computationally obtained results for $(P_1^{\text{bubble}}, P_0)$ with different values of τ_0 in the stabilization parameter $\tau_K = \tau_0 h_K$ are shown in Fig. 1. As mentioned earlier, see the discussion at the end of Sect. 4, when the τ_0 decreases the tendency of smearing out and when it increases oscillations in the numerical solution are observed. For example, in the case of $\tau_0 = 0.00045$, the solution becomes very smooth, and in the case of $\tau_0 = 0.045$, the solution starts to oscillate, see Fig. 1 top and middle, respectively. For an optimal (numerically tuned) value of $\tau_0 = 0.0045$, the boundary layer is captured very well in the local projection method, see Fig. 1 (bottom).

The obtained numerical results for $(P_2^{\text{bubble}}, P_1^{\text{disc}})$ with different values of τ_0 in $\tau_K = \tau_0 h_K$ are presented in Fig. 2. Here, the behavior of the numerical solution with respect to the stabilization parameter τ_0 is opposite to the linear element (P_1^{bubble}) case. That is, for a small value of $\tau_0 = 0.003$ the solution oscillates, and for a large value of $\tau_0 = 0.012$, the tendency of smearing out is observed, see Fig. 2 top and middle, respectively. This opposite behaviour of smearing and oscillations of the P_1 part of the solution can be explained in case of a one-dimension model problem, see [28]. For this second order element P_2^{bubble}, an optimal value of $\tau_0 = 0.006$ (numerically tuned) captures the boundary layer very well, see Fig. 2 (bottom).

7.2 Example 2

Let $\Omega = (0,1)^2$, $\epsilon = 10^{-8}$, $b(x,y) = (-y,x)^{\mathrm{T}}$, $c = 0$, $\Gamma_N := \{0\} \times (0,1)$ and $f = 0$ be in (7). On the outflow boundary, we impose the homogeneous Neumann condition, i.e.,

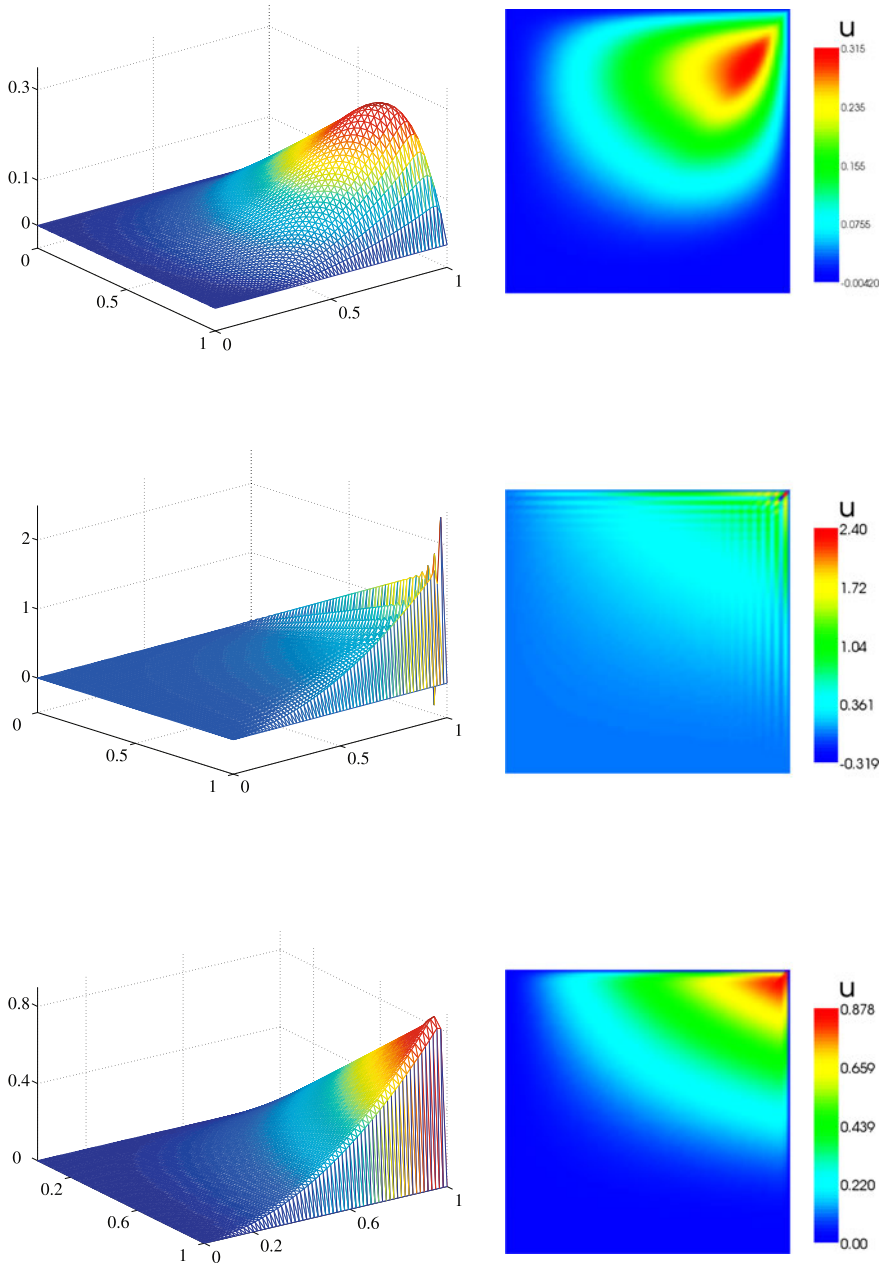

Fig. 1 Solution of Example 1 for P_1^{bubble} with projection onto P_0. The stabilization parameter values are $\tau_0 = 0.00045$ (*top*), 0.045 (*middle*), and 0.0045 (*bottom*)

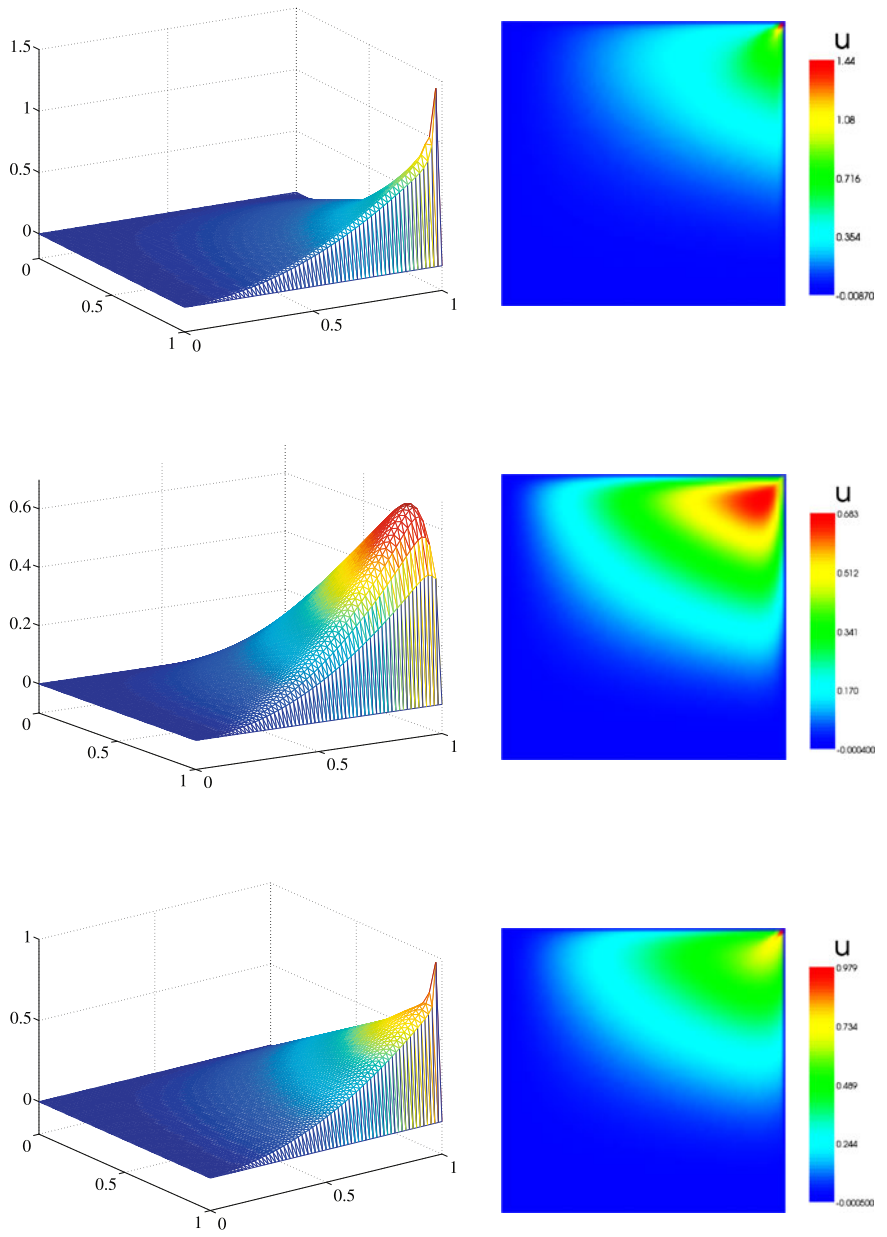

Fig. 2 Solution of Example 1 for P_2^{bubble} with projection onto P_1^{disc}. The stabilization parameter values are τ_0=0.003 (*top*), 0.012 (*middle*), and 0.006 (*bottom*)

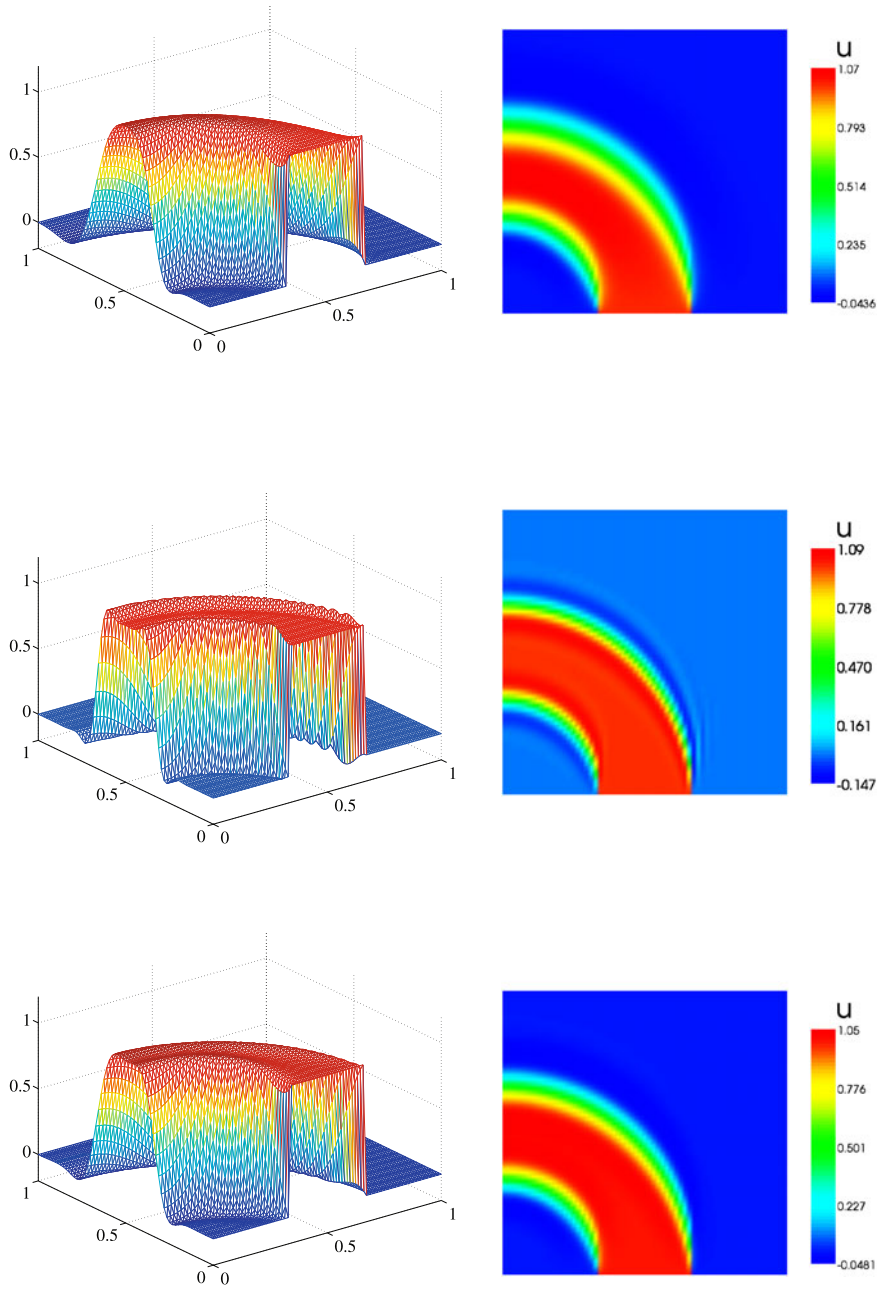

Fig. 3 Solution of Example 2 for P_1^{bubble} with projection onto P_0. The stabilization parameter values are $\tau_0 = 0.00045$ (*top*), 0.045 (*middle*), and 0.0045 (*bottom*)

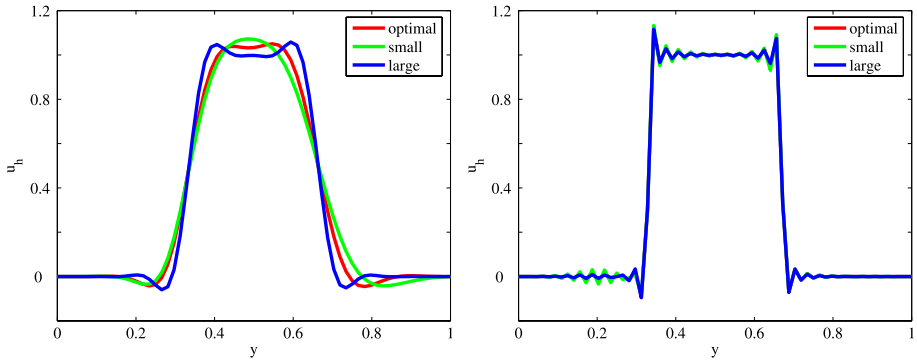

Fig. 4 Solution of Example 2 at the outflow boundary part for P_1^{bubble} with projection onto P_0 (*left*) and P_2^{bubble} with projection onto P_1^{disc} (*right*). The stabilization parameter values are $\tau_0 = 0.00045$ (small), 0.045 (large), and 0.0045 (optimal)

$g = 0$. Further, we prescribe the discontinuous Dirichlet data

$$u_D(x, y) = \begin{cases} 1 & \text{if } (x, y) \in (1/3, 2/3) \times \{0\}, \\ 0 & \text{else} \end{cases}$$

on Γ_D. This discontinuous Dirichlet data is transported counter-clockwise to the homogeneous Neumann outflow boundary.

In this example, the triangulation and the number of degrees of freedom are same as in Example 1. The obtained numerical results for the piecewise linear element $(P_1^{\text{bubble}}, P_0)$ with different values of τ_0 are presented in Fig. 3. Here, we take the same stabilization parameter values used in the Example 1. In this example, the influence of the stabilization parameter τ_0 on the solution is very less. Moreover, for small and large τ_0 values, there is only a small difference in the solution, see Fig. 3. However, as in the Example 1, the tendency of smearing out when τ_0 decreases, and the solution starts to oscillate when τ_0 increases is observed for $(P_1^{\text{bubble}}, P_0)$.

To compare the effect of the linear and higher order elements, the numerically obtained solution at the outflow boundary for $(P_1^{\text{bubble}}, P_0)$ and $(P_2^{\text{bubble}}, P_1^{\text{disc}})$ elements are presented in Fig. 4.

7.3 Example 3

Let $\Omega = (-3, 9) \times (-3, 3) \setminus \{(x, y) \in \mathbb{R}^2;\ x^2 + y^2 \leq 1\}$, $\epsilon = 10^{-8}$, $b(x, y) = (1, 0)^{\mathrm{T}}$, $c = 0$, $\Gamma_N := \{9\} \times (-3, 3)$ and $f = 0$ be in (7). On the out flow boundary, we impose the homogeneous Neumann condition, i.e., $g = 0$. The Dirichlet data

$$u_D(x, y) = \begin{cases} 1 & \text{if } x^2 + y^2 = 1, \\ 0 & \text{else} \end{cases}$$

is prescribed on Γ_D. This example is having two inner layers along $(0, 9) \times \{\pm 1\}$ and a boundary layer along the curve $x \leq 1$, $x^2 + y^2 = 1$.

To solve this example, we use two types of triangulation: (i) inner layer unresolved mesh, (ii) inner layer resolved mesh, see Fig. 5. In both cases, (i) and (ii), we used 32,944 and

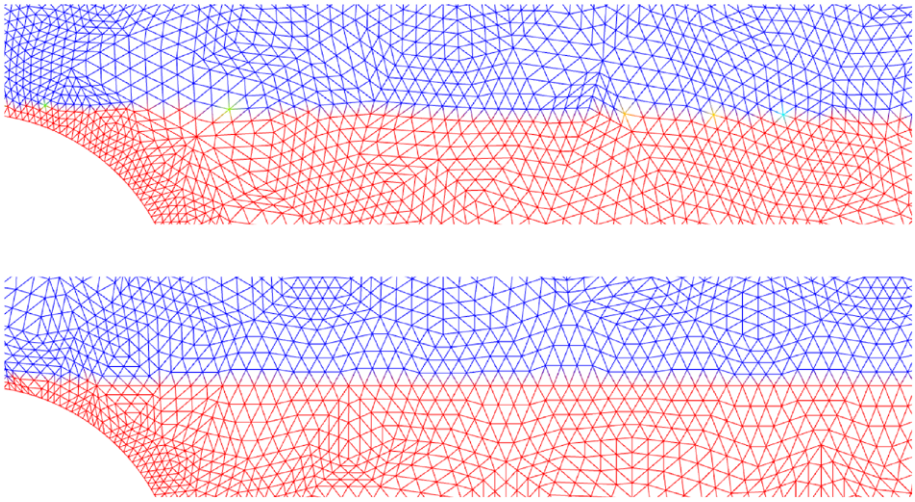

Fig. 5 Unresolved mesh (*top*) and resolved mesh (*bottom*) in the neighbourhood of $y = 1$ used in Example 3

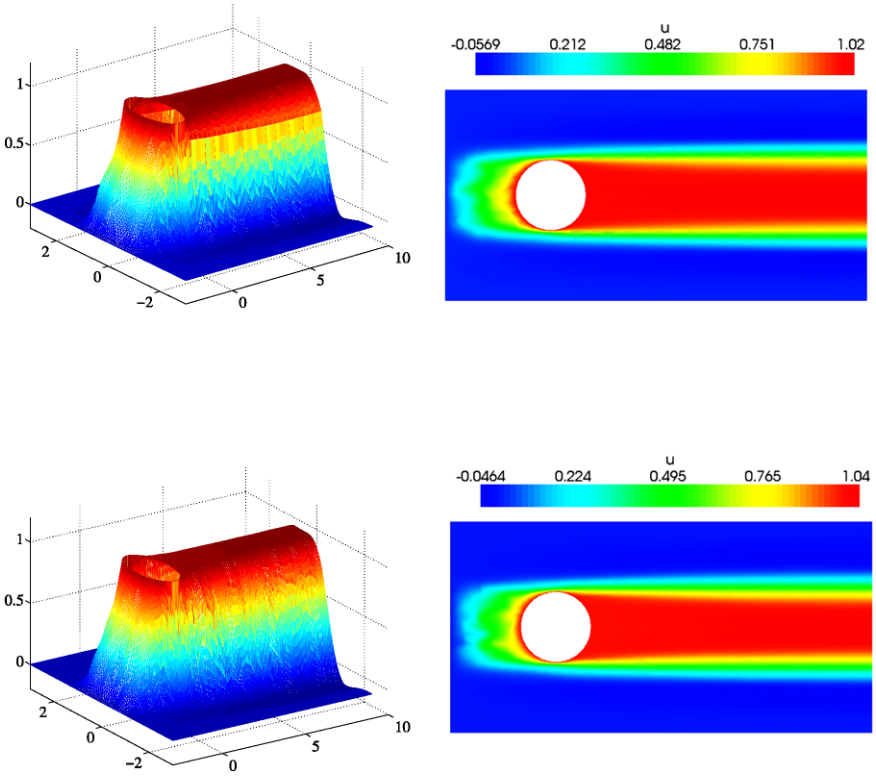

Fig. 6 Solution of Example 3 for P_1^{bubble} with projection onto P_0. Computations are performed for inner layer unresolved mesh (*top*) and inner layer resolved mesh (*bottom*)

31,344 triangles, respectively. For the piecewise linear elements, these result in 49,742 and 47,342 degrees of freedom, respectively. In these computations, we take $\tau_0 = 0.0045$, which is the optimal value in Example 1. The obtained numerical results are shown in Fig. 6. The numerical oscillations in the solutions is about 5% in these computations even for very small $\epsilon = 10^{-8}$. Further, the influence of inner layer unresolved and resolved meshes is very small.

Acknowledgement The authors like to thank the DFG for partly supporting the research in this paper by grant To143/9 and Andreas Hahn for performing the numerical computations.

References

1. Baiocchi, C., Brezzi, F., Franca, L.P.: Virtual bubbles and GaLS. Comput. Methods Appl. Mech. Eng. **105**, 125–142 (1993)
2. Becker, R., Braack, M.: A finite element pressure gradient stabilization for the Stokes equations based on local projections. Calcolo **38**(4), 173–199 (2001)
3. Becker, R., Braack, M.: A two-level stabilization scheme for the Navier–Stokes equations. In: Feistauer, M., Dolejší, V., Knobloch, P., Najzar, K. (eds.) Numerical Mathematics and Advanced Applications, pp. 123–130. Springer, Berlin (2004)
4. Braack, M., Burman, E.: Local projection stabilization for the Oseen problem and its interpretation as a variational multiscale method. SIAM J. Numer. Anal. **43**, 2544–2566 (2006)
5. Braack, M., Burman, E., John, V., Lube, G.: Stabilized finite element methods for the generalized Oseen problem. Comput. Methods Appl. Mech. Eng. **196**, 853–866 (2007)
6. Brezzi, F., Marini, D., Russo, A.: Applications of the pseudo residual-free bubbles to the stabilization of convection–diffusion problems. Comput. Methods Appl. Mech. Eng. **166**, 51–63 (1998)
7. Brezzi, F., Russo, A.: Choosing bubbles for advection–diffusion problems. Math. Models Methods Appl. Sci. **4**, 571–587 (1994)
8. Brooks, A.N., Hughes, T.J.R.: Streamline upwind/Petrov–Galerkin formulations for convection dominated flows with particular emphasis on the incompressible Navier–Stokes equations. Comput. Methods Appl. Mech. Eng. **32**, 199–259 (1982)
9. Burman, E.: A unified analysis for conforming and nonconforming stabilized finite element methods using interior penalty. SIAM J. Numer. Anal. **43**, 2012–2033 (2005)
10. Burman, E., Ern, A.: Continuous interior penalty hp-finite element methods for advection and advection-diffusion equations. Math. Comput. **76**, 1119–1140 (2007)
11. Burman, E., Fernandez, M.A., Hansbo, P.: Continuous interior penalty finite element method for Oseen's equations. SIAM J. Numer. Anal. **44**, 1248–1274 (2006)
12. Burman, E., Hansbo, P.: Edge stabilization for Galerkin approximations of convection-diffusion-reaction problems. Comput. Methods Appl. Mech. Eng. **193**, 1437–1453 (2004)
13. Ern, A., Guermond, J.-L.: Theory and Practice of Finite Elements. Applied Mathematical Sciences, vol. 159. Springer, New York (2004)
14. Franca, L.P., Frey, S.L.: Stabilized finite element methods: II. The incompressible Navier–Stokes equations. Comput. Methods Appl. Mech. Eng. **99**, 209–233 (1992)
15. Franca, L.P., Russo, A.: Recovering SUPG using Petrov–Galerkin formulations enriched with adjoint residual-free bubbles. Comput. Methods Appl. Mech. Eng. **182**, 333–339 (2000)
16. Ganesan, S., Matthies, G., Tobiska, L.: Local projection stabilization of equal order interpolation applied to the Stokes problem. Math. Comput. **77**, 2039–2060 (2008)
17. Girault, V., Raviart, P.-A.: Finite Element Methods for Navier–Stokes Equations. Springer Series in Computational Mathematics, vol. 5. Springer, Berlin (1986)
18. Guermond, J.-L.: Stabilization of Galerkin approximations of transport equations by subgrid modeling. Math. Model. Numer. Anal. **33**, 1293–1316 (1999)
19. Hughes, T.J.R., Franca, L.P., Balestra, M.: A new finite element formulation for computational fluid dynamics. V: Circumventing the Babuška–Brezzi condition: A stable Petrov–Galerkin formulation of the Stokes problem accommodating equal-order interpolations. Comput. Methods Appl. Mech. Eng. **59**, 85–99 (1986)
20. Matthies, G., Skrzypacz, P., Tobiska, L.: A unified convergence analysis for local projection stabilisations applied to the Oseen problem. Math. Model. Numer. Anal. **41**, 713–742 (2007)
21. Nävert, U.: A finite element method for convection-diffusion problems. Ph.D. thesis, Chalmers University of Technology, Göteborg (1982)

22. Ohmori, K., Ushijima, T.: A technique of upstream type applied to a linear nonconforming finite element approximation of convective diffusion equation. RAIRO Numer. Anal. **18**, 309–332 (1984)
23. Roos, H.-G., Stynes, M., Tobiska, L.: Numerical Methods for Singularly Perturbed Differential Equations. Convection–Diffusion and Flow Problems. Springer, Berlin (1996)
24. Schieweck, F., Tobiska, L.: A nonconforming finite element method of upstream type applied to the stationary Navier–Stokes equations. RAIRO Numer. Anal. **23**, 627–647 (1989)
25. Schieweck, F., Tobiska, L.: An optimal order error estimate for an upwind discretization of the Navier–Stokes equations. Numer. Methods Partial Differ. Equ. **12**, 107–127 (1996)
26. Tabata, M.: A finite element approximation corresponding to the upwind differencing. Memoirs Numer. Math. **1**, 47–63 (1977)
27. Tabata, M., Fujima, S.: An upwind finite element scheme for high Reynolds-number flow. Int. J. Numer. Methods Fluids **12**, 305–322 (1991)
28. Tobiska, L.: On the relationship of local projection stabilization to other stabilized methods for one-dimensional advection–diffusion equations. Comput. Methods Appl. Mech. Eng. doi:10.1016/j.cma.2008.10.016 (2008)
29. Tobiska, L., Verfürth, R.: Analysis of a streamline diffusion finite element method for the Stokes and Navier–Stokes equations. SIAM J. Numer. Anal. **33**, 407–421 (1996)